

Modeling pressure drop of inclined flow through a heat exchanger for aero-engine applications

D. Missirlis^a, K. Yakinthos^{a,*}, P. Storm^b, A. Goulas^a

^a *Laboratory of Fluid Mechanics and Turbomachinery, Department of Mechanical Engineering,
Aristotle University of Thessaloniki, Thessaloniki 54 124, Greece*

^b *MTU Aero Engines GmbH, Dachauerstrasse 665, 80995 München, Germany*

Received 4 January 2006; received in revised form 23 June 2006; accepted 23 June 2006

Available online 7 September 2006

Abstract

In the present work further numerical predictions for the flow field through a specific type of a heat exchanger, which is planned to be used in the exhaust nozzle of aircraft engines. In order to model the flow field through the heat exchanger, a porous medium model is used based on a simple quadratic relation, which connects the pressure drop with the inlet air velocity in the external part of the heat exchanger. The aim of this work is to check the applicability of the quadratic law in a variety of velocity inlet conditions configured by different angles of attack. The check is performed with CFD and the results are compared with new available experimental data for these inlet conditions. A detailed qualitative analysis shows that although the quadratic law has been derived for a zero angle of attack, it performs very well for alternative non-zero angles. These observations are very helpful since this simple pressure drop law can be used for advanced computations where the whole system of the exhaust nozzle together with the heat exchangers can be modeled within a holistic approach.

© 2006 Elsevier Inc. All rights reserved.

Keywords: Heat exchanger; Aero engine applications; Porous medium; Flow angle; Pressure drop

1. Introduction

We present additional experimental and numerical investigations for the inclined flow field through a heat exchanger developed by MTU Aero Engines. The basic concept of the heat exchanger has been already described in previous works of Missirlis et al. (2005) and Schönenborn et al. (2004). During the numerical modeling, the heat exchanger has been modeled with the use of an isotropic porous medium. Based on our experimental data, it has been proven that the pressure drop is following a polynomial law, Eq. (1), having one linear and one quadratic term, an assumption, which is in accordance with the fundamental conclusions found in the international literature.

$$\Delta P_{\text{static, exp}} = 7.171 V_{\text{eff}}^2 + 10.088 V_{\text{eff}} \text{ [Pa]} \quad (1)$$

In the real operating conditions, the role of the heat exchanger is to transfer energy from the exhaust hot gas back to the combustor. This transfer is performed by a system of heat exchangers which are installed in the exhaust nozzle located downstream the aero engine. Due to the whole setup of the heat exchangers, the hot gas passes through the exchangers having various angles of attack. In this work the quadratic law derived for the specific heat exchanger, for zero angle of attack Missirlis et al. (2005) is tested for non-zero angles of attack. The tests are performed with CFD and the numerical results are compared with new available experimental data. A detailed qualitative analysis shows that although, the quadratic law has been derived for a zero angle of attack, it performs very well for alternative non-zero angles.

2. The experimental setup

A model of the heat exchanger has been constructed and mounted in the test section of a wind tunnel. Two sets of

* Corresponding author.

E-mail address: kyros@eng.auth.gr (K. Yakinthos).

Nomenclature

H	width of test section
P_{static}	static pressure
P_{total}	total pressure
V_{eff}	effective velocity
V_{magn}	velocity magnitude
V_x	axial velocity component – normal to the heat exchanger

V_z spanwise velocity component – parallel to the heat exchanger

Greek letter

$\Delta P_{\text{static,exp}}$ static pressure drop derived from experimental measurements

measurements have been carried out for angle of attack equal to 15° and 45° corresponding to inlet mass flows equal to 1.76 and 1.63 kg/s, respectively. For each angle

of attack, pressure and velocity measurements have been carried out upstream and downstream the heat exchanger following the same experimental method as in the work of Missirlis et al. (2005).

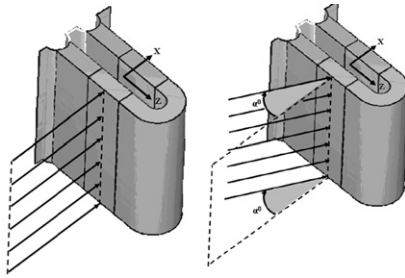


Fig. 1. Definition of zero (left) and non-zero (right) angle of attack.

Table 1

Pressure drop error for the different grids and different non-zero angles of attack

Grid	Computational cells	Time (h)	15° 1.76 kg/s		45° 1.63 kg/s	
			ΔP_{total} error (%)	ΔP_{static} error (%)	ΔP_{total} error (%)	ΔP_{static} error (%)
1	450,000	120	−0.48	−0.52	1.39	2.36
2	115,000	24	−0.58	−0.66	1.92	2.92
3	30,000	6	−1.02	−1.07	2.84	3.47

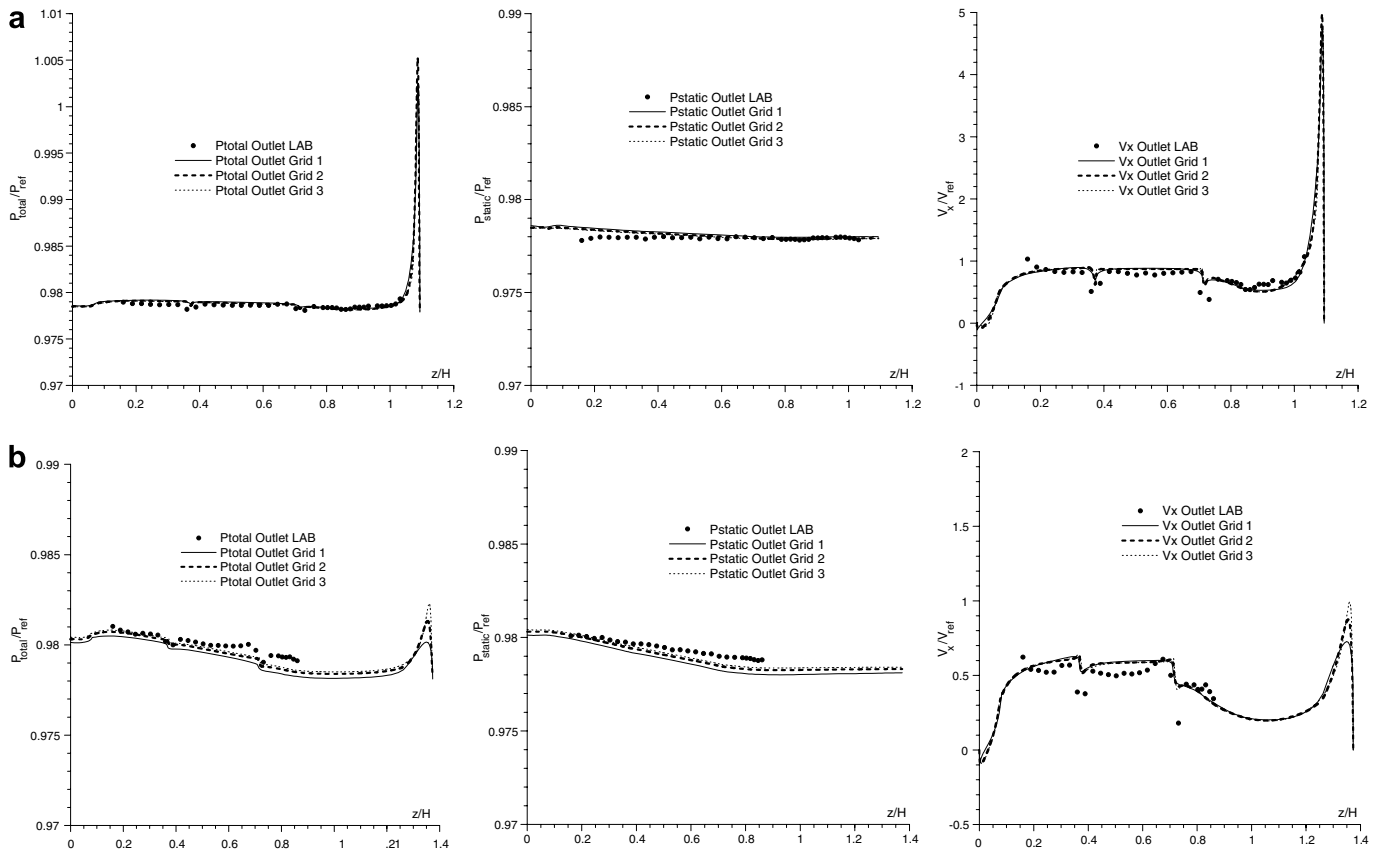


Fig. 2. (a) Case of 15° and (b) case of 45° . Comparison between experimental data (dots) and numerical results for the outlet section of the heat exchanger.

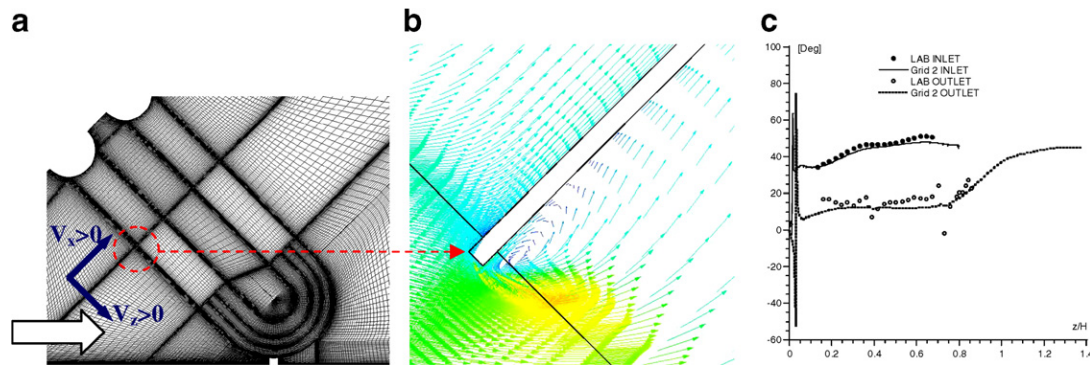


Fig. 3. Case of 45° (Grid 2): (a) Picture of the computational grid; (b) vector plot of the flow field developing in the near region of the spacer plates and (c) comparison of the flow angle at the inlet and outlet section.

3. The computational modeling of the heat exchanger

The general pressure drop law Equation (1) is adopted to a numerical modeling procedure. For both cases of non-zero angles of attack, three meshes have been constructed ranging from 30,000 to 450,000 computational cells. Following the conclusions of our previous work and for the inlet conditions of the experiments, the characteristic Reynolds numbers are equal to 2918 and 3207 for 15° and 45° angle of attack, respectively, indicating that the flow lies within the transitional regime and, more specifically, closer to the laminar regime as stated by the work of Umeda and Yang (1999). The numerical modeling has been performed by using the commercial CFD package FINE™ (2003) by NUMECA Int. The quadratic pressure drop law has been treated as an extra source term in the 2D Navier–Stokes equations. The convergence criterion for the solved flow variables has been chosen to be less or equal to 10^{-5} .

4. Discussion of the numerical results

Comparisons between the CFD results and the 3-D experimental measurements are presented in Fig. 2 and Table 1. The experimental data in Fig. 2 have been “plane averaged” in order to obtain the appropriate information for the comparisons with the 2-D numerical approach. The pressure is non-dimensionalized by the average static pressure, P_{static} , while the velocity by the average velocity magnitude, V_{magn} , equal to $\sqrt{V_x^2 + V_z^2}$, at the inlet section of the heat exchanger. The spanwise direction is non-dimensionalized by the width H of the test section. As it can be seen, the three grids show in general an adequate grid independency in the largest part of the spanwise direction for both cases of non-zero angle of attack and present satisfactory numerical predictions compared to the experimental measurements.

A careful investigation of the numerical results shows that the porous medium model adopted for the pressure drop is capable to predict sufficiently the pressure distribution, a conclusion which is supported by the results of Table

1, where it is shown that the average pressure drop error is relatively low for the two angles of attack and for all three grids. The results tend to be improved and stabilized as the number of points used is increased. Thus, it can be concluded that for both cases the results are in acceptable accordance with the experimental measurements and can be judged as being sufficiently accurate.

A small exception exists in the regions near the wind tunnel sidewalls, left and right limit of the abscissa, where the results are more sensitive to the grid quality due to the development of the collector’s pipes wake and sidewall boundary layer. However, since the primary goal of this work was the investigation of the behavior of the pressure drop law towards the angle of attack, the results in the wake regions were regarded as sufficiently accurate and no further investigation was needed for these regions specifically.

In Fig. 3(b) a detailed view of the region of the spacer plates is presented, which helps in the understanding of the flow field development. It is clearly shown that the air-flow enters in a direction non-parallel to the exchanger, caused by the non-zero angle of attack, but after a small distance, is developed to a direction, which is parallel to the orientation of the heat exchanger. Undoubtedly, the spacer plates contribute significantly to this behavior. This development is also noticed in the regions away from the spacer plates, as it can be seen in Fig. 3(c) where a significant flow alignment is observed despite the fact that the outlet section is located at significant distance downstream of the heat exchanger. Thus, it can be concluded that the spacers together with the tube arrangement (Fig. 1 in Missirlis et al. (2005), in the real installation, also helps the flow to align and to pass finally through the heat exchanger with an almost zero angle of attack.

5. Conclusions

From the comparisons between computational results and experimental data it can be concluded that an adoption of a relatively simple quadratic law for the pressure drop through this specific type of heat exchanger can be applied.

The numerical results have been compared with new available experimental data for non-zero angles of attack and showed quite satisfactory agreement, especially for the pressure drop, a flow parameter, that is, of primary interest since it can affect the operation of the turbo-compressor located upstream the heat exchanger. It has been observed that the heat exchanger geometry contributes to a great extent to the adoption of this simple pressure drop law since, some distance after the first tube rows, the airflow becomes aligned to the exchanger and, thus, develops in a similar condition as for the zero angle of attack.

Unfortunately, this modeling procedure cannot be applied to any arbitrary type of heat exchanger. But the general concept can help when there is a need to model, by means of CFD, the flow development through devices, which have installed heat exchangers. One can measure the pressure drop for a variety of mass flows in a small part of the exchanger (upstream and downstream of the heat exchanger) for a relatively simple to setup inlet condition (zero angle of attack) and then proceed to the derivation of the pressure drop law.

A possible future approach could be the adoption of a more advanced pressure drop law by introducing other flow parameters that surely affect the losses through the heat exchanger. Since in the real operating conditions the flow is compressible and there is also a large amount of heat transfer, a more sophisticated law should encounter the effects of temperature variations together with the density and viscosity variations. As indicated by [Antohe et al.](#)

(1997) the validity of a quadratic pressure drop law decreases as the flow moves away from the velocity range, which was used for the determination of the coefficients values.

Acknowledgments

The experimental part of this work has been financially supported by the E.U. under the “Competitive and Sustainable Growth Programme”, Contact No. G4RD-CT-1999-00069.

References

- Antohe, B.V., Lage, J.L., Price, D.C., Weber, R.M., 1997. Experimental determination of permeability and inertia coefficients of mechanically compressed aluminum porous matrices. *ASME J. Fluids Eng.* 119, 404–412.
- FINETM Numeca's Flow Integrated Environment. User Manual, ver. 6.1-1, February 2003.
- Missirlis, D., Yakinthos, K., Palikaras, A., Katheder, K., Goulas, A., 2005. Experimental and numerical investigation of the flow field through a heat exchanger for aero-engine applications. *Int. J. Heat Fluid Flow* 26, 440–458.
- Schönenborn, H., Simon, B., Ebert, E., Storm, P., 2004. Thermomechanical design of a heat exchanger for a recuperative aero engine. In: *Proceedings of ASME Turbo Expo 2004, Power for Land, Sea and Air*.
- Umeda, S., Yang, S.W., 1999. Interaction of von Karman vortices and intersecting main streams in staggered tubes bundles. *Exp Fluids* 26, 389–396.